Ion-Kinetic-Energy Measurements and Energy Balance in a *Z*-Pinch Plasma at Stagnation

E. Kroupp, D. Osin, A. Starobinets, V. Fisher, V. Bernshtam, and Y. Maron
Weizmann Institute of Science, Rehovot 76100, Israel

I. Uschmann and E. Förster
Friedrich-Schiller University, Jena, Germany

A. Fisher
Faculty of Physics, Technion-Israeli Institute of Technology, Haifa, Israel

C. Deeney
Sandia National Laboratories, Albuquerque, New Mexico, USA
(Received 3 November 2006; published 14 March 2007)

The ion-kinetic energy throughout *K* emission in a stagnating plasma was determined from the Doppler contribution to the shapes of optically thin lines. X-ray spectroscopy with a remarkably high spectral resolution, together with simultaneous imaging along the pinch, was employed. Over the emission period, a drop of the ion-kinetic energy down to the electron thermal energy was seen. Axially resolved time-dependent electron-density measurements and absolute intensities of line and continuum allowed for investigating, for the first time, each segment of the pinch, the balance between the ion-kinetic energy at the stagnating plasma, and the total radiation emitted. Within the experimental uncertainties, the ion-kinetic energy is shown to account for the total radiation.

DOI: 10.1103/PhysRevLett.98.115001 PACS numbers: 52.58.Lq, 52.70.La

In *Z*-pinch experiments [1] the magnetic field energy delivered to the plasma during the implosion is mainly stored in the form of plasma-kinetic energy. At stagnation (as the plasma assembles on axis) this energy is converted into plasma internal energy and radiation. In principle, at stagnation, additional energy may be delivered to the plasma by the magnetic field, and, in turn, part of the ion-kinetic energy may not be converted to radiation, but rather spent on plasma flows or on thermal convection to neighboring plasmas. The process of the energy conversion to radiation is of fundamental importance, including phenomena such as shock waves and magnetohydrodinamic turbulence, that are of general implications for laboratory plasmas and astrophysics.

Z pinches have been studied extensively [1] due to their high relevance to inertial confinement fusion, to x-ray radiation sources, and to the study of matter under high energy density. However, satisfactory understanding of the balance between the imploding plasma-kinetic energy, and radiation at stagnation is still lacking, and is considered to be a central problem in the present *Z*-pinch research [1–4]. A long-standing problem is the balance between the kinetic energy of that part of the plasma that stagnates on axis at the end of the implosion phase and the total radiation emitted at stagnation. It had been pointed out, in particular, that the radiation energy may exceed the ion-kinetic energy [2,4,5]. Detailed experimental investigations of the ion-kinetic energy throughout the stagnation phase is thus of great importance for improving the understanding of *Z*-pinch stagnation dynamics. Investigations of ion velocities from Doppler contributions to *K* lines were reported in a few studies [6–9], where in Ref. [9] the enhancement of the radiation energy relative to the total ion-kinetic energy is addressed.

Here we report on a time-resolved determination of the ion-kinetic energy in the stagnating *K*-emitting plasma, in a neon-puff experiment. In ''kinetic energy'' we here refer to the total ion-kinetic energy (thermal and hydrodynamic). Because of the satisfactory reproducibility of the discharges, measurements for different times in different experiments allowed for tracking the ion-kinetic-energy history throughout the entire *K* emission period.

Such measurements can be performed if Doppler-dominated emission-line spectral shapes are observed. A principal requirement, therefore, is that the line shapes are not affected by opacity (while the lines are sufficiently intense to allow for a satisfactory accuracy) or by Stark broadening. Furthermore, the instrumental spectral resolution has to be high enough, which, for these experiments, required a resolution of $\lambda/\Delta\lambda \approx 6400$. Also, the spectroscopic systems should allow for a simultaneous imaging of the pinch column along its axis, which allows for a separate data analysis for each Δz segment. Because of the common nonuniformities along the column, this feature, together with targeting all other spectroscopic observations to the same segment, were decisively needed for reaching the conclusions here below.

To determine the total number of ions depositing their kinetic energy at the given pinch segment, we measured the axially resolved time-dependent electron-density, plasma radial extent, line and continuum intensities, and total *K* radiation. Using detailed atomic-kinetics modeling, this

yielded the histories of the electron-temperature and the radiating-plasma mass.

Here, we do not address the total energy balance of the imploding plasma or the mechanisms of the ion-kinetic-energy conversion at stagnation. Rather, the data allow for a local comparison between the total ion-kinetic energy at the K-emitting plasma at stagnation and the total energy radiated from that plasma. It is shown that at the beginning of the K emission the radiating ion-kinetic energy is comparable to that expected at the end of the implosion phase, dropping later to a value comparable to the electron temperature at the stagnating plasma. It is, in particular, demonstrated that the ion-kinetic energy deposited at the K-emitting plasma, may account for the total energy radiated from this plasma.

The imploding gas in the present experiments ($\approx$20 μg/cm) was injected by a nozzle 38 mm in diameter. Following Ref. [10], an additional nozzle delivering $\approx$4 μg/cm on axis was used, which led to a substantial increase in the K emission. The implosion time was $\approx$750 ns and the current at stagnation was $\approx$320 kA.

The crystal used for this study is a spherically curved potassium acid phthalate operated at the second order. Double-grating measurements verified that the crystal true rocking curve is only $\approx$10% broader than the theoretical one, giving a Lorentzian spectral response with a width measured to be 1.8 mÅ (corresponding to $\lambda/\Delta\lambda \approx$ 6700). Employing a high dispersion on the detector plane allowed for obtaining a resolving power $\approx$6400 for the spectrograph. Instrumental broadening due to the pinch size is negligible in the present measurements, as verified by ray-tracing simulations. The spectra were viewed in the radial direction and the spherical shape of the crystal allowed for both obtaining spectra imaging along the z axis with a spatial resolution down to 0.1 mm and for collecting sufficient number of photons. A single-gated microchannel plate (MCP) detector coupled to a CCD camera provides $\approx$ 1-ns temporal resolution throughout the 10-ns K emission period.

To measure the Doppler profiles in the stagnation phase, the crystal was designed to focus on the three Ly_α satellites: $2p^2{}^1D_2 - 1s2p^1P_1$, $2s2p^3P_{0,1,2} - 1s2s^3S_1$, and $2p^2{}^3P_{0,1,2} - 1s2p^3P_{0,1,2}$, where one is a singlet transition (12.355 Å) that is most useful for the observation of the Doppler broadening [11]. For our plasma parameters, the singlet line natural broadening is determined by the rates of the upper-level autoionization (3.7×10^{14} s^{-1}) and radiative decay (1.2×10^{13} s^{-1}), giving a width of 3.3 mÅ. This Lorentzian broadening, together with the instrumental response, give for the measurements a Lorentzian spectral response of FWHM = 5.1 mÅ. As seen in the calculations discussed below, the singlet-satellite upper level is populated by dielectronic recombination (rather than by inner-shell excitations), meaning that the singlet-satellite shapes give the H-like (rather than the He-like) ion-kinetic energy.

The K emission was found to begin at the segment z = 9–12 mm, where $z = 0$ and $z = 14.4$ mm are the cathode and anode positions, respectively; see Fig. 1. Also for this segment, the K emission remained nearly uniform throughout the emission period. In this Letter, we only discuss the measurements for this segment.

Figure 2(a) shows the Ly_α-satellite structure observed near $z = 10.5$ mm at an early time of the K emission period, i.e., at $t = -3$ ns relative to the peak time of the total K emission signal observed from the z = 9–12 mm segment using a filtered absolutely calibrated photoconductive detector (PCD) [12]. In obtaining the Doppler contribution we assume that this contribution is Gaussian. We thus fit Voigt profiles to each of the satellite components, where the Gaussian part is a parameter determined by the best fit and the Lorentzian part is known, as discussed above.

Assuming each component of the other triplet satellites has the same width as the singlet satellite (consistent with Doppler-dominated widths), the structure of all satellites was constructed satisfactorily [Fig. 2(a)]. For the early time of the stagnation, the widths obtained for the Gaussian contributions to the profiles of the singlet satellite are 8–11 mÅ (much larger than the system spectral resolution). The satellite structures observed later in the stagnation [Fig. 2(b)] demonstrates much smaller FWHM for the Gaussian contribution, 2.5 $\pm$ 0.6 mÅ. Figure 3 shows the Gaussian FWHM values for the z = 9–12 mm segment; error bars shown are mainly due to the shot irreproducibility. Since at stagnation it is highly plausible that the ion velocity distribution is nearly isotropic in 3D, these values are used to infer an effective ion temperature $T_i^{\text{eff}}(t)$ that serves to give the total ion-kinetic energy $E_k^{\text{ion}} = 3/2T_i^{\text{eff}}$, see Fig. 3.

The radiating H-like ions thus have a kinetic energy $\approx$ 3.4 keV early at stagnation, dropping to $\approx$0.3 keV later,

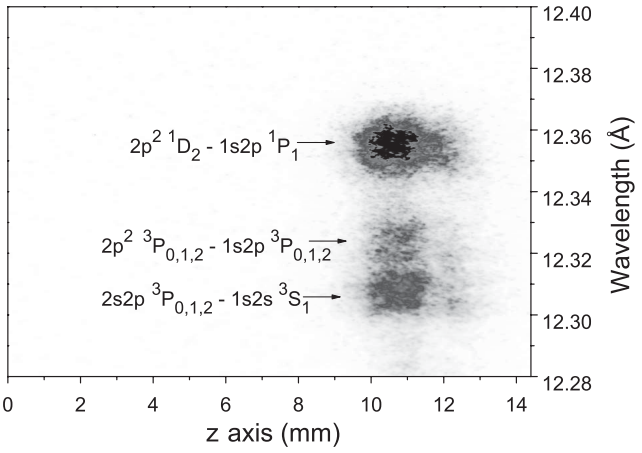

FIG. 1. The Ly_α satellites imaged in the z direction, observed at $t = -3$ ns (relative to the PCD-signal peak time) with a 2-ns-gate MCP camera. The cathode and anode surfaces are located at $z = 0$ and $z = 14.4$ mm, respectively.

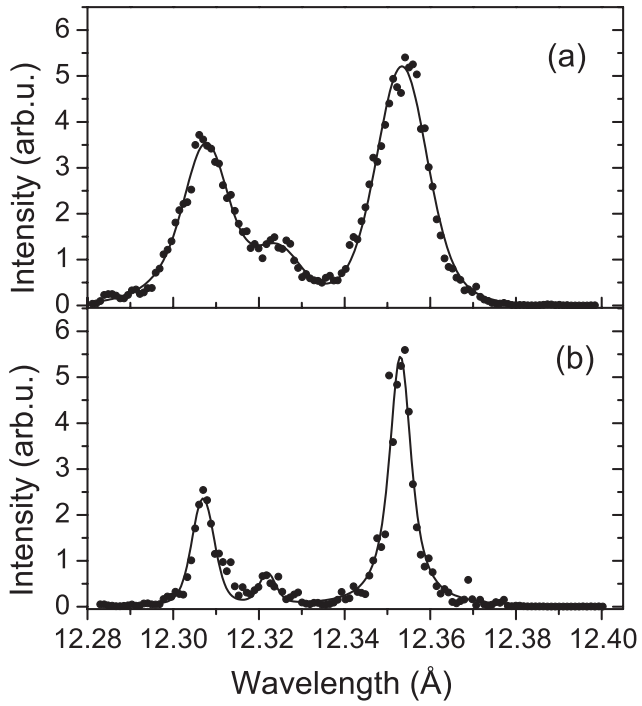

FIG. 2. (a) Satellite spectrum integrated over 9.7–11.3 mm for $t = -3$ ns. The best fit gives a Gaussian with a FWHM of 11 mÅ; (b) Satellite spectrum integrated over 9.9–10.1 mm for $t = +6$ ns. The best fit gives a Gaussian with a FWHM of 2.5 mÅ.

the latter being comparable to the electron thermal energy $(3/2kT_e)$ determined independently, see below.

Together with the atomic-kinetics modeling described below, the data are also used to obtain the time-resolved electron-density n_e of the H-like plasma, based on the n_e dependence of the triplet-satellite intensity ratio [11]. It was found that n_e in the H-like plasma is $\approx(2 \pm 1) \times 10^{20}$ cm^{-3}, nearly constant during the emission period.

The PCD measurement (Fig. 4) yielded 15 J for the total K radiation from the considered segment. Also, the absolute intensity of the continuum above the H-like edge (at 1.58–1.82 keV) was determined using Ross filters [13]. The continuum optical thinness makes its intensity highly useful for determining the radiating-plasma mass. The Ross filters were also used to obtain the time-dependent absolute Ly_α intensity, which, using a spectrograph that provided Ly_α and its satellites simultaneously, yielded the satellite absolute intensity.

Finally, four-frame (1-ns gates with 1.5-ns interframe time) filtered pinhole photography showed that the radius of the K-emitting plasma (of the $z = 9$–12 mm segment) starts rising from a value ≈ 0.1 mm at $t \approx -5$ ns to a peak value ≈ 0.45 mm at $t \approx 0$, followed by a drop until the end of the emission. A rise in the radiating-plasma radius, while the density remains nearly constant, was also seen in high-current wire-array experiments [14].

The analysis of the energy balance requires information on the histories of the mass, electron temperature, and ion

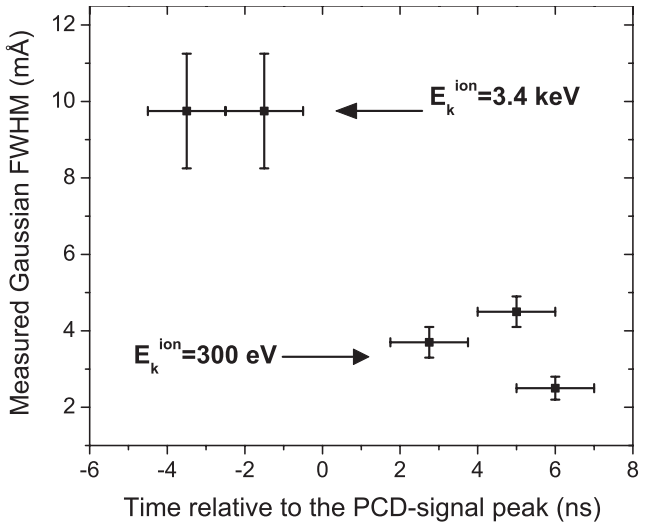

FIG. 3. The FWHM of the Gaussian contributions to the singlet-satellite shapes as a function of time, obtained from spectra integrated over segments 0.2 to 0.6 mm long near $z = 10.5$ mm, and averaged over 3–5 shots. Also indicated are the corresponding ion kinetic energies.

composition of the radiating plasma. This is obtained from the measurements described above with the aid of the following modeling [15]: the stagnating plasma is assumed to be a uniform cylinder with a radius $R(t)$, $n_e(t)$, and $T_e(t)$. Our time-dependent collisional radiative calculations account for the radiation transport self-consistently. They are used for the determination of the time-dependent level populations, optical coefficients, and radiation flux onto each of the detectors. For the emissivity and opacity we use spectral line shapes based on the observed Doppler broadening. For $R(t)$ in the modeling we use the pinhole photography data and for n_e we assume a constant value, as measured.

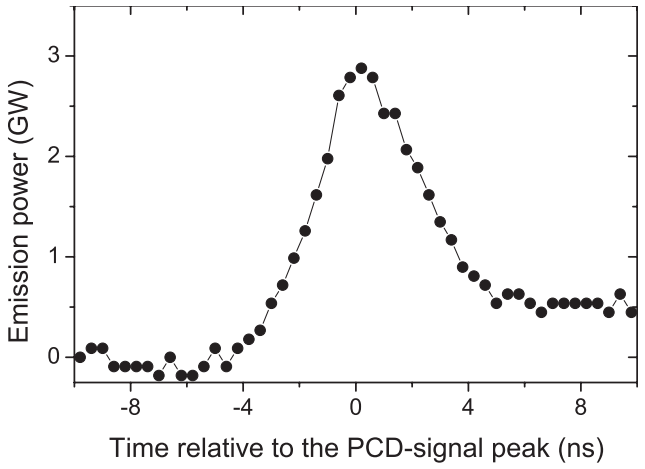

FIG. 4. Radiation power (at $h\nu \geq 0.7$ keV) measured by a PCD, integrated over $z = 9$ to $z = 12$ mm of the pinch column, corrected for the 7.5-μm-thick Be filter.

For $T_e(t)$, as an input parameter, we use a smooth function that rises and drops during the stagnation period, and is determined by fitting to the data. $T_e(t)$ is rather tightly constrained by fitting the peak times of the satellite ($t \approx 0$) and continuum ($t \approx +3$ ns) intensities. Also in the modeling, n_e and $R(t)$ are repeatedly varied within the measurement uncertainties, in order to obtain best fits to the absolute time-dependent K emission, continuum signals, and to the absolute time-resolved satellite intensities, which also serves to obtain the uncertainties. The modeling yields that T_e in the H-like plasma rises from a value of $\approx$150 eV at $t = -4$ ns, peaks at $\approx$250 eV at $t \approx 0$ ns, and then drops to 80–140 eV at $\approx +6$ ns. The modeling also confirms the optical thinness of the Ly_α satellites ($\tau < 0.1$). It is also gives that the peak K-emitting mass M_{peak} (the mass at $t = 0$) is 5 ± 2.5 μg/cm. The time dependence of T_e and of the charge-state distribution obtained by the modeling is also used to estimate the change in the ionization energy and the electron thermal energy. This yields a drop in these energies of 0.6 ± 0.8 keV/ion during the K emission, plausibly assumed to be converted to the K radiation.

We now obtain the total energy available for conversion to radiation for the considered plasma segment. Let us assume that each of the ions contributing to the K radiation from the $z = 9$–12 mm pinch segment loses a kinetic energy similar to that seen for the H-like ions. The kinetic energy lost by each ion is thus 3.1 ± 0.8 keV/ion (see Fig. 3). Adding the energy gained by the plasma due to the recombination and electron cooling (see above), yields that the total energy available for the total radiation is $E^{\text{total}} = 3.7 \pm 1.1$ keV/ion.

This value should be compared to the total radiation per ion in the stagnating plasma. Note that measuring the total radiation emitted is not useful due to the soft radiation from the surrounding halo plasmas. Thus, we use the measured K radiation shown in Fig. 4, together with our best-fit modeling, to obtain the total energy, including the soft emission ($h\nu < 0.7$ keV), radiated from the stagnating plasma. Correction is also made for possible little absorption of the K emission in the halo plasmas. This gives 21 ± 5 J for $z = 9$–12 mm (70 ± 15 J/cm). Assuming that the number N_i of the ions that contribute to the radiation is given by M_{peak}, yields that the radiated energy $\epsilon_{\text{rad}}/N_i$ is 3.3 ± 1.4 keV/ion. Thus, while the process of the ion energy conversion is still far from being understood, for the present experiment, and under the assumption of the modeling of a radially and axially uniform plasma within the $z = 9$–12 mm segment, it appears that the kinetic energy of the ions at the stagnating plasma, together with the ionization and electron thermal energy in the plasma, are sufficient to account for the total radiation energy during the stagnation period.

We note, however, that while this experiment demonstrates that the ion-kinetic energy in the stagnating plasma explains the energy radiated from the plasma, it does not preclude the possibility that additional energy may be delivered to the plasma by the magnetic field, since in turn energy may also be lost by the plasma not through radiation, e.g., by plasma flows or thermal convection. Detailed understanding of the Z-pinch-stagnation dynamics requires further combined experimental and computational studies, including comparisons to higher-current or wire-array experiments.

We thank M. Cuneo for reading the manuscript and J. Apruzese, J. Bailey, R. Commisso, J. Davis, M. Desjarlais, Yu. Ralchenko, A. Velikovich, and K. Whitney for valuable discussions. We thank P. Meiri for skilled assistance. This work was supported by the German-Israeli Project Cooperation, by the DOE Center for High-Energy-Density Studies, and by the Israel Science Foundation.

[1] *Dense Z-Pinches*, edited by J. Chittenden (AIP, Oxford, United Kingdom, 2006).
[2] C. Deeney, P. D. LePell, B. H. Failor, S. L. Wong, J. P. Apruzese, K. G. Whitney, J. W. Thornhill, J. Davis, E. Yadlowsky, and R. C. Hazelton *et al.*, Phys. Rev. E **51**, 4823 (1995).
[3] D. L. Peterson, R. L. Bowers, K. D. McLenithan, C. Deeney, G. A. Chandler, R. B. Spielman, M. K. Matzen, and N. F. Roderick, Phys. Plasmas **5**, 3302 (1998).
[4] A. L. Velikovich, J. Davis, J. W. Thornhill, J. L. Giuliani, L. I. Rudakov, and C. Deeney, Phys. Plasmas **7**, 3265 (2000).
[5] K. G. Whitney, J. W. Thornhill, J. P. Apruzese, J. Davis, C. Deeney, and C. A. Coverdale, Phys. Plasmas **11**, 3700 (2004).
[6] T. W. L. Sanford, T. J. Nash, R. C. Mock, R. B. Spielman, K. W. Struve, J. H. Hammer, J. S. D. Groot, K. G. Whitney, and J. P. Apruzese, Phys. Plasmas **4**, 2188 (1997).
[7] K. L. Wong, P. T. Springer, J. H. Hammer, C. A. Iglesias, A. L. Osterheld, M. E. Foord, H. C. Bruns, J. A. Emig, and C. Deeney, Phys. Rev. Lett. **80**, 2334 (1998).
[8] E. J. Yadlowsky, F. Barakat, E. P. Carlson, R. C. Hazelton, M. Keitz, C. C. K. B. H. Failor, J. S. Levine, Y. Song, B. L. Whitten, and C. R. Coverdale *et al.*, J. Appl. Phys. **92**, 3458 (2002).
[9] M. G. Haines, P. D. LePell, C. A. Coverdale, B. Jones, C. Deeney, and J. P. Apruzese, Phys. Rev. Lett. **96**, 075003 (2006).
[10] T.-F. Chang, A. Fisher, and A. V. Drie, J. Appl. Phys. **69**, 3447 (1991).
[11] J. F. Seely, Phys. Rev. Lett. **42**, 1606 (1979).
[12] Provided by P. D. LePell (Sandia National Laboratories).
[13] E. Kroupp, A. Starobinets, E. Klodzh, Y. V. Ralchenko, Y. Maron, I. N. Bogatu, and A. Fisher, J. Appl. Phys. **92**, 4947 (2002).
[14] J. Bailey and P. D. LePell (private communication).
[15] V. I. Fisher, D. V. Fisher, and Y. Maron, High Energy Density Physics (to be published).